Hydrol. Earth Syst. Sci. Discuss., 12, 5789–5840, 2015
www.hydrol-earth-syst-sci-discuss.net/12/5789/2015/
doi:10.5194/hessd-12-5789-2015

Hydrology and Earth System Sciences
Discussions
Open Access

South Asia river flow projections and their implications for water resources

C. Mathison[1], **A. J. Wiltshire**[1], **P. Falloon**[1], **and A. J. Challinor**[2]

[1]Met Office Hadley Centre, FitzRoy Road, Exeter, EX1 3PB, UK
[2]School of Earth and Environment, Institute for Climate and Atmospheric Science, University of Leeds, Leeds, LS2 9AT, UK

Received: 16 April 2015 – Accepted: 29 April 2015 – Published: 16 June 2015

Correspondence to: C. Mathison (camilla.mathison@metoffice.gov.uk)

Published by Copernicus Publications on behalf of the European Geosciences Union.

Abstract

South Asia is a region with a large and rising population and a high dependance on industries sensitive to water resource such as agriculture. The climate is hugely variable with the region relying on both the Asian Summer Monsoon (ASM) and glaciers for its supply of fresh water. In recent years, changes in the ASM, fears over the rapid retreat of glaciers and the increasing demand for water resources for domestic and industrial use, have caused concern over the reliability of water resources both in the present day and future for this region. The climate of South Asia means it is one of the most irrigated agricultural regions in the world, therefore pressures on water resource affecting the availability of water for irrigation could adversely affect crop yields and therefore food production. In this paper we present the first 25 km resolution regional climate projections of river flow for the South Asia region. ERA-Interim, together with two global climate models (GCMs), which represent the present day processes, particularly the monsoon, reasonably well are downscaled using a regional climate model (RCM) for the periods; 1990–2006 for ERA-Interim and 1960–2100 for the two GCMs. The RCM river flow is routed using a river-routing model to allow analysis of present day and future river flows through comparison with river gauge observations, where available.

In this analysis we compare the river flow rate for 12 gauges selected to represent the largest river basins for this region; Ganges, Indus and Brahmaputra basins and characterize the changing conditions from east to west across the Himalayan arc. Observations of precipitation and runoff in this region have large or unknown uncertainties, are short in length or are outside the simulation period, hindering model development and validation designed to improve understanding of the water cycle for this region. In the absence of robust observations for South Asia, a downscaled ERA-Interim RCM simulation provides a benchmark for comparison against the downscaled GCMs. On the basis that these simulations are among the highest resolution climate simulations available we examine how useful they are for understanding the changes in water resources for the South Asia region. In general the downscaled GCMs capture the seasonality of the river flows, with timing of maximum river flows broadly matching the available observations and the downscaled ERA-Interim simulation. Typically the RCM simulations over-estimate the maximum river flows compared to the observations probably due to a positive rainfall bias and a lack of abstraction in the model although comparison with the downscaled ERA-Interim simulation is more mixed with only a couple of the gauges showing a bias compared with the downscaled GCM runs. The simulations suggest an increasing trend in annual mean river flows for some of the river gauges in this analysis, in some cases almost doubling by the end of the century; this trend is generally masked by the large annual variability of river flows for this region. The future seasonality of river flows does not change with the future maximum river flow rates still occuring during the ASM period, with a magnitude in some cases, greater than the present day natural variability. Increases in river flow during peak flow periods means additional water resource for irrigation, the largest usage of water in this region, but also has implications in terms of inundation risk. Low flow rates also increase which is likely to be important at times of the year when water is historically more scarce. However these projected increases in resource from rivers could be more than countered by changes in demand due to reductions in the quantity and quality of water available from groundwater, increases in domestic use due to a rising population or expansion of other industries such as hydro-electric power generation.

1 Introduction

South Asia, the Indo-Gangetic plain in particular, is a region of rapid socio-economic change where both population growth and climate change is expected to have a large impact on available water resource and food security. The region is home to almost 1.6 billion people and the population is forecast to increase to more than 2 billion by 2050 (United Nations, 2013). The economy of this region is rural and highly dependant on climate sensitive sectors such as the agricultural and horticultural industry, characterised by a large demand for water resources. As a result, over the coming decades, the demand for water from all sectors; domestic, agricultural and industrial is likely to increase (Gupta and Deshpande, 2004; Kumar et al., 2005).

The climate of South Asia is dominated by the Asian Summer Monsoon (ASM), with much of the water resource across the region provided by this climatological phenomena during the months of June–September (Goswami and Xavier, 2005). The contribution from glacial melt to water resources is less certain but likely to be important outside the ASM period during periods of low river flow (Mathison et al., 2013). Glaciers and seasonal snowpacks are natural hydrological buffers releasing water during spring and autumn when the flows of catchments like the Ganges are at their lowest. Similarly they may act to buffer inter-annual variability as well releasing water during warmer drier years and accumulating during wetter colder years (Barnett et al., 2005). Recent studies have shown that both of these are changing (ASM rainfall – Christensen et al., 2007, and glacier mass balance – Fujita and Nuimura, 2011) putting more pressure on groundwater resources which is not sustainable in the longer term (Rodell et al., 2009). Gregory et al. (2005) suggest that the availability and quality of ground water for irrigation could be more important factors influencing food security than the direct effects of climate change, particularly for India. Aggarwal et al. (2012) suggest that an increase in extremes (both temperature and precipitation) could lead to instability in food production and it is this variability in food production that is potentially the most significant effect of climate change for the South Asia region.

Immerzeel et al. (2010) found that by the 2050s the main upstream water supply could decrease by approximately 18 % although this decrease was partly offset by an 8 % increase in precipitation. Immerzeel et al. (2010) use general circulation models (GCMs) which have a coarse resolution and are known to have difficulty in capturing the monsoon precipitation and in estimating the relationship between daily mean temperature and melting of snow and ice.

The Indo-Gangetic plains have traditionally provided the staple crops of rice and wheat (Aggarwal et al., 2000) for India and South Asia as a whole, irrigation is an important part of this industry and any limitation of water resource needed to maintain yields of these crops could have implications on the food and water security of the region. The aim of this analysis is to examine how useful these simulations are for understanding how river flows could change in South Asia in the future and the implications this could have on water resources that are increasingly in demand. The water resources for the South Asia region as a whole are generally poorly understood with limitations in the observing networks and availability of data for both precipitation and river flows presenting a real challenge for validating models and estimates of the water balance of the region. In this analysis we use a 25 km resolution regional climate model (RCM) with a demonstrated ability to capture the ASM to downscale ERA-interim re-analysis data (Simmons et al., 2007) and two GCMs able to capture the main features of the large-scale circulation (Annamalai et al., 2007; Mathison et al., 2013). In the absence of robust observations, particularly for high elevation regions like the Himalaya, the ERA-interim simulation provides a constrained estimate of the water balance of the region. In a previous study, Akhtar et al. (2008) found that RCM data produced better results when used with a hydrological model than using poor-quality observation data; this implies greater confidence in the RCM simulated meteorology than available observational data for this region (Wiltshire, 2013). Therefore in this analysis, as in Wiltshire (2013), in addition to the observations that are available, it is appropriate to use the ERA-interim simulation as a benchmark against which to evaluate the GCM driven regional simulations. The RCM includes a land-surface model which includes a full physical energy-balance snow model (Lucas-Picher et al., 2011) providing an estimate of the gridbox runoff which is then used to drive the Total Runoff Integrating Pathways river routing model (TRIP; Oki and Sud, 1998) in order to present 25 km resolution regional climate projections of riverflow for the South Asia region. TRIP has been used previously in Falloon et al. (2011) which used GCM outputs directly to assess the skill of a global river-routing scheme. TRIP is applied here to runoff from a subset of the 25 km resolution RCM simulations completed as part of the EU HighNoon project (HNRCM) to provide river flow rates for South Asia. A selection of river flow gauges, mainly from the GRDC (GRDC, 2014) network provide observations which are used, in addition to downscaled ERA-interim river flows, to evaluate the downscaled GCM river flows for the major catchments of the South Asia region; these river gauges aim to illustrate from the perspective of river flows as modelled in an RCM, that the influence of the ASM on precipitation totals increases, from west to east and north to south across the Himalayan mountain range, while that of western disturbances reduces (Wiltshire, 2013; Dimri et al., 2013; Ridley et al., 2013; Collins et al., 2013). The differing influences across the Himalayan arc result in complex regional differences in sensitivity to climate change; with western regions dominated by non-monsoonal winter precipitation and therefore potentially less susceptible to reductions in annual snowfall (Wiltshire, 2013; Kapnick et al., 2014). The selection of these gauges and the models used are described in Sect. 2, while a brief evaluation of the driving data and the river flow analysis is presented in Sect. 3. The implications of the potential changes in river flows on water resources and conclusions are discussed in Sects. 4 and 5 respectively.

2 Methodology

2.1 Observations

The total precipitation within each of the downscaled GCM simulations are compared against a downscaled ERAinterim simulation and precipitation observations from the Asian Precipitation-Highly Resolved Observational Data Integration Towards the Evaluation of Water Resources (APHRODITE – Yatagai et al., 2012) dataset in Sect. 3.1 focusing on the main river basins in the region and included in the river flow analysis (in Sect. 3.2); the Indus and the Ganges/Brahmaputra. The precipitation patterns for each basin are useful for understanding the changes in the river flows within the catchments, however, rain gauges in the APHRODITE dataset are particularly sparse at higher elevations (see Yatagai et al., 2012, Fig. 1) which leads to underestimation of the basin wide water budgets particularly for mountainous regions (Andermann et al., 2011). Therefore the reanalysis product ERAinterim (Simmons et al., 2007) is also used as a benchmark to compare the downscaled GCMs against. All of the gauges selected for the river flow analysis presented here lie within these river catchments and are chosen to characterize the conditions along the Himalayan arc using river flow data from the Global Runoff Data Centre (GRDC, 2014). A brief geographical description of the rivers and the chosen gauges is given in this section, their locations are shown in Fig. 1 and listed in Table 1 (including the abbreviations shown in Fig. 1 and the gauge location in terms of latitude and longitude).

The Indus, originates at an elevation of more than 5000 m in western Tibet on the northern slopes of the Himalayas, flowing through the mountainous regions of India and Pakistan to the west of the Himalayas. The upper part of the Indus basin is greatly influenced by western disturbances which contribute late winter snowfall to the largest glaciers and snow fields outside the polar regions; the meltwaters from these have a crucial role in defining the water resource of the Indus basin (Wescoat Jr., 1991). In this analysis the Attock gauge is the furthest upstream and the Kotri gauge, located further downstream provide observations on the main trunk of the Indus river. The Chenab river, located in the Panjnad basin and in this analysis represented by the Panjnad gauge, is a major eastern tributary of the Indus, originating in the Indian state of Himachal Pardesh. In the upper parts of the Chenab sub-basin western disturbances contribute considerably to precipitation while the foothills are also influenced by the ASM (Wescoat Jr., 1991).

The Ganges river originates on southern slopes of the Himalayas (Thenkabail et al., 2005) and traverses thousands of kilometres before joining with the Brahmaputra in Bangladesh and emptying into the Bay of Bengal (Mirza et al., 1998). The Ganges basin has a population density 10 times the global average making it the most populated river basin in the world (Johnston and Smakhtin, 2014), it covers

1.09 million km^2 with 79 % in India, 13 % in Nepal, 4 % in Bangladesh and 4 % in China (Harding et al., 2013). The main trunk of the Ganges is represented in this analysis by the gauge at the Farakka barrage, located at the India–Bangladeshi border, to the East of the Himalayas. The Bhagirathi river, located in the region often referred to as the Upper Ganga basin, is one of the main head streams of the Ganges. The Bhagirathi river originates from Gaumukh 3920 m a.s.l. at the terminus of the Gangotri glacier in Uttarakhand, India (Bajracharya and Shrestha, 2011). The Tehri dam is located on this tributary, providing the most central data point on the Himalayan arc in this analysis (this is not a GRDC gauge).

The Karnali river (also known as Ghaghara), drains from the Himalaya originating in Nepal flowing across the border to India where it drains into the Ganges. The Karnali is the largest river in Nepal and a major tributary of the Ganges (Bajracharya and Shrestha, 2011) accounting for approximately 11 % of the Ganges discharge, 5 % of its area and 12 % of its snowfall in the HNRCMs. Two of the river gauges in this analysis; the Benighat and the Chisapani are located on this river. Two other sub-catchments complete those covering the Ganges basin; the Narayani river (also known as the Gandaki River, represented here by the Devghat river gauge); reportedly very dependant on glaciers at low flow times of the year with over 1700 glaciers covering more than 2200 km^2 (Bajracharya and Shrestha, 2011). The Arun river, part of the Koshi river basin originates in Tibet, flows south through the Himalayas to Nepal. The Arun, represented in this analysis by the Turkeghat gauge joins the Koshi river which flows in a southwest direction as a tributary of the Ganges.

The Brahmaputra originates from the glaciers of Mount Kailash at more than 5000 m a.s.l., on the northern side of the Himalayas in Tibet flowing into India, and Bangladesh before merging with the Padma in the Ganges Delta. The Brahmaputra is prone to flooding due to its surrounding orography and the amount of rainfall the catchment receives (Dhar and Nandargi, 2000). The Brahmaputra is represented in this analysis by three gauges; Yangcun, the highest upstream gauge, Pandas in the middle and Bahadurabad furthest downstream but above the merge with the Padma.

2.2 Models

This analysis utilizes 25 km resolution regional climate modelling of the Indian subcontinent to provide simulations across the Hindu-Kush Karakoram Himalaya mountain belt. To sample climate uncertainty, two GCM simulations that have been shown to capture a range of temperatures and variability in precipitation similar to the AR4 ensemble for Asia (Christensen et al., 2007) and that have been shown to simulate the ASM (Kumar et al., 2013; Annamalai et al., 2007); The Third version of the Met Office Hadley Centre Climate Model (HadCM3 – Pope et al., 2000; Gordon et al., 2000, a version of the Met Office Unified Model) and ECHAM5 (3rd realization – Roeckner et al., 2003) are downscaled using the HadRM3 (Jones et al., 2004) RCM. An ERA-interim (Simmons et al., 2007) driven RCM simulation is also shown to provide a benchmark for comparison against the GCM driven simulations in the absence of good quality observations (see Sects. 2.1 and 3.1). The RCM simulations are performed at 25 km, part of the ensemble produced for the EU-HighNoon program, for the whole of the Indian subcontinent (25° N, 79° E–32° N, 88° E) and are currently the finest resolution modelling available for this region (Mathison et al., 2013; Moors et al., 2011; Kumar et al., 2013). There are 19 atmospheric levels and the lateral atmospheric boundary conditions are updated 3 hourly and interpolated to a 150 s timestep. The experimental design of the HighNoon ensemble compromises between the need for higher resolution climate information for the region, the need for a number of ensemble members to provide a range of uncertainty and the limited number of GCMs that are able to simulate the ASM. These factors are all important given the limited computational resources available.

In these simulations the land surface is represented by version 2.2 of the Met Office Surface Exchange Scheme (MOSESv2.2, Essery et al., 2003). MOSESv2.2 treats subgrid land-cover heterogeneity explicitly with separate surface temperatures, radiative fluxes (long wave and shortwave), heat fluxes (sensible, latent and ground), canopy moisture contents, snow masses and snowmelt rates computed for each surface type in a grid box (Essery et al., 2001). However the air temperature, humidity and wind speed above the surface are treated as homogenous across the gridbox and precipitation is applied uniformly over the different surface types of each gridbox. The relationship between the precipitation and the generation of runoff is complicated, depending on not only the intensity, duration and distribution of the rainfall but also the characteristics of the surface e.g. the infiltration capacity of the soil, the vegetation cover, steepness of the orography within the catchment and the size of the catchment (Linsley et al., 1982). In GCMs and even 25 km RCMS such as the ones presented here, the resolution is often too coarse to explicitly model the large variations of soil moisture and runoff within a catchment and therefore the major processes are parameterized (Gedney and Cox, 2003). The method used within MOSES2.2 for generating surface and subsurface runoff across a gridbox is through partitioning the precipitation into interception by vegetation canopies, throughfall, runoff and infiltration for each surface type (Essery et al., 2003). The Dolman and Gregory (1992) infiltration excess mechanism generates surface runoff; this assumes an exponential distribution of point rainfall rate across the fraction of the catchment where it is raining (Clark and Gedney, 2008). Moisture fluxes are allowed between soil layers; these are calculated using the Darcy equation, with the water going into the top layer defined by the gridbox average and any excess removed by lateral flow (Essery et al., 2001). Excess moisture in the bottom soil layer drains from the bottom of the soil column at a rate equal to the hydraulic conductivity of the bottom layer as subsurface runoff (Clark and Gedney, 2008). The performance of MOSESv2.2 is discussed in the context of a GCM in Essery et al. (2001), however no formal assessment of MOSESv2.2 and the runoff generation in particular has been done for the RCM.

In this analysis the simulated runoff is converted into river flow using the TRIP river routing scheme (Oki and Sud, 1998) as a post-processing step. TRIP is a simple model that moves water along a pre-defined 0.5° river network; the Simulated Topological Network at 30 min resolution (STN-30p, version 6.01; Vörösmarty et al., 2000a, b; Fekete et al., 2001) in order to provide mean runoff per unit area of the basin which can be compared directly with river gauge observations. The TRIP model has been shown to agree well with observed river flow gauge data (Oki et al., 1999) and largely showed good skill when comparing run off from several land surface models (Morse et al., 2009). Implementation of TRIP in two GCMs; HadCM3 and HadGEM1 is described by Falloon et al. (2007) and was found to improve the seasonality of the river flows into the ocean for most of the major rivers. Using TRIP ensures the river flow forcing is consistent with the atmospheric forcing, however it also assumes that all runoff is routed to the river network and as such there is no net aquifer recharge/discharge. This may not be the case in regions with significant ground water extraction which is subsequently lost though evaporation and transported out of the basin. These simulations do not include extraction, which for this region is large, particularly for irrigation purposes (Biemans et al., 2013); this means that the extraction-evaporation and subsequent recycling of water in a catchment (Harding et al., 2013; Tuinenburg et al., 2014) is not considered in this analysis. The routed runoff of the HNRCM simulations are referred to here using only the global driving data abbreviations; ERAint, ECHAM5 and HadCM3.

3 Results

3.1 Comparison of present day driving data with observations

In this section we summarise the main points from previous analysis and evaluation of the HNRCM simulations that provide the driving data for the river flow projections (Kumar et al., 2013; Lucas-Picher et al., 2011; Mathison et al., 2013). We also look again at the total precipitation for these simulations focussing on the major river basins for the region before presenting the river flow projections for individual gauges in Sect. 3.2. Lucas-Picher et al. (2011) evaluates the ability of RCMs to capture the ASM using ERA-40 data, Kumar et al. (2013), as part of the HighNoon project, completes analysis using the HNRCMs forced with ERA-Interim data. The HNRCM simulations are themselves evaluated against a range of observations for the Ganges/Brahmaputra river basin in Mathison et al. (2013). Figure 2 shows the spatial distribution of total precipitation for the monsoon period (June to September; Goswami and Xavier, 2005) for APHRODITE observations together with the downscaled ERAint and GCM driven simulations. Figure 2 highlights that, in general the HNRCM simulations capture the spatial characteristics of the ASM, successfully reproducing regions of high convective precipitation, maximum land rainfall and the rain shadow over the east coast of India as described in more detail in Kumar et al. (2013). The RCMs are also able to reproduce the inter-annual variability of the region although they underestimate the magnitude of the variation (Kumar et al., 2013). In general the GCMs in the AR4 ensemble exhibit cold and wet biases compared to observations both globally (Nohara et al., 2006) and for South Asia (Christensen et al., 2007), although these are generally reduced in the RCM simulations there is a cold bias in the RCM that is probably carried over from the larger bias in the GCMs (Mathison et al., 2013; Kumar et al., 2013).

Figures 3 and 4 show the annual mean and the monthly climatology of the total precipitation for the RCM simulations, compared with 25 km resolution APHRODITE observations, for the main basins in this analysis; the Indus and the Ganges/Brahmaputra. The Ganges and Brahmaputra catchments are considered together in this analysis as these rivers join together in the Ganges Delta and within TRIP there is no clear delineation between the two catchments. In general the models appear to over estimate the seasonal cycle of total precipitation (Fig. 4) compared with the APHRODITE observations; this is highlighted by the annual mean of the total precipitation shown in Fig. 3. However, the sparsity of the observations at high elevations dicussed in Sect. 2.1 make it difficult to attach error bars to the observations particularly for mountainous regions and therefore an ERAint simulation is used to provide a benchmark for comparison against the two downscaled GCM simulations. The annual mean (Fig. 3) and the monthly climatology (Fig. 4) show that, for these catchments, the ERAint simulation lies between the two HighNoon ensemble members except during peak periods of precipitation when the magnitude of the total precipitation in the ERAint simulation is larger.

The seasonal cycles of total precipitation are distinctly different between the basins shown. The Indus basin (Fig. 4, left), indicates two periods of precipitation; one smaller peak between January and May and another larger one between July and September. The smaller peak occurs later than both ERAint and the observations for the downscaled GCM simulations while the timing of the larger peak compare well between the observations, ERAint and the downscaled GCM simulations. The magnitude of the peaks in precipitation in the APHRODITE observations are consistently lower throughout the year than the simulations. The magnitude of the ERAint total precipitation is typically larger than both GCM driven simulations while the ECHAM5 simulation is the lowest and closest to the APHRODITE observations, HadCM3 is between ECHAM5 and ERAint for most of the year. In contrast the Ganges/Brahmaputra catchment (Fig. 4, right) has one strong peak between July and September; this cycle is also captured reasonably well by the simulations, both in terms of magnitude and timing of the highest period of precipitation. However there is a tendancy for the simulations to overestimate rainfall between January and June compared to the observations, thus lengthening the wet season (Mathison et al., 2013). Mathison et al. (2013) also show that in these simulations, the region of maximum precipitation along the Himalayan foothills is displaced slightly to the north of that shown in the observations. One explanation for this could be that the peak in total precipitation is due the distribution of observations already discussed. Alternatively it could be due to the model resolution, which may, at 25 km still be too coarse to adequately capture the influence of the orography on the region of maximum precipitation and therefore it is displaced from where it actually occurs. The downscaled ERAint simulation also indicates a higher total precipitation for January–May that is within the range of uncertainty of the GCM driven simulations. However for the remainder of the Monsoon period, ERAint has a higher total precipitation than the GCM driven simulations; this is highlighted by the spatial distribution of total precipitation shown in Fig. 2 which shows that ERAint has a slightly larger and more intense area of maximum rainfall over the Eastern Himalayas than shown in the observations.

3.2 Present day modelled river flows

In this section we compare present day modelled river flows with observations and a downscaled ERAint simulation using annual average river flows (see Fig. 5) and monthly climatologies (see Fig. 6).

The annual average river flow rates for each river gauge (described in Sect. 2.1) are shown by the paler lines in Fig. 5 (red line-HadCM3, blue line-ECHAM5) with the darker lines showing a smoothed average to highlight any visible trends in the simulations. The plots show the model data for the whole period of the simulations including the historical period for each of the simulations and the available observations (GRDC, 2014 – black line) for that location. It is clear from this plot that observed river flow data is generally limited which makes statistical analysis of the observations difficult. River flow data for this region is considered sensitive and is therefore not readily available particularly for the present day. For each of the gauges shown here, there are generally several complete years of data but often the time the data was collected pre-dates the start of the model run. The ERAint simulation is also shown (cyan line-ERAint) to provide a benchmark in the absence of well-constrained observations (See Sect. 3.1). The comparison between the model and observations shown in Figs. 5 and 6 is therefore to establish if the model and observations are comparable in terms of the average seasonal cycle and mean river flow rate without over-interpreting how well they replicate the observations.

The multi-year monthly mean modelled river flows for ECHAM5 (blue line), HadCM3 (red line), for the period 1971–2000 and ERAint (cyan line) for the period 1990–2007 are shown for each river gauge location in Fig. 6. The multi-year mean for all the available observations are also shown (Fig. 6, black line – GRDC (2014) except for the Tehri Dam on the Bhagirathi river for which observations are not shown but were received via personal communication from the Tehri Dam operator). The shaded regions show the 1.5 standard deviation (SD) from the mean for each GCM driven model for the 1971–2000 period which represents the variability of the region and provides a plausible range of river flows in the absence of any known observation errors for the GRDC observations (personal communication, GRDC). Estimates of observation errors for river gauges vary in the literature with a recommendation in Falloon et al. (2011) for GCMs to be consistently within 20 % of the observations while Oki et al. (1999) suggest that errors of 5 % at the 95 % confidence interval might be expected. McMillan et al. (2010) propose a method for quantifying the uncertainty in river discharge measurements by defining confidence bounds. Therefore in this analysis, where the 1.5 SD range encompasses the observations and ERAint, given the variability of the region and the limitations of the observations, this is considered a reasonable approximation.

The Kotri gauge on the Indus (Fig. 6, 1st row, left column) and the Yangcun gauge on the Brahmaputra (Fig. 6, 6th row, left column) are the only two gauges where the modelled river flow is higher than the observations and not within the estimated variability (1.5 SD) of the region. The ERAint simulation is also outside the estimated variability (1.5 SD) for the Benighat gauge on the Karnali river (Fig. 6, 3rd row, left column). The differences in these gauges are also reflected in the annual mean river flows (Fig. 5) for these river gauges which are higher than observed. The explanation for the river flow at the Kotri gauge being too high could be due to the extraction of water which is not included in the model; this is particularly plausible for this gauge as this is a downstream gauge located relatively close to the river mouth and the Indus has a relatively large extraction rate (Biemans et al., 2013). The Yangcun gauge is a more upstream gauge and the differences between the model and observations for this gauge are more likely to be related to the precipitation in the simulations which is high at this location, particularly during the ASM (see Fig. 2); this could be having a direct effect on the riverflow.

At the other two gauges on the Brahmaputra downstream of the Yangcun gauge; the Pandu and Bahadurabad (Fig. 6, 6th row, right column and 5th row, right column respectively), the seasonal cycle of river flow has a very broad peak particularly in the modelled river flows compared to the other gauges. In the simulations the snowfall climatology for the Ganges/Brahmaputra basin (not shown) has a similar seasonal cycle to that of the river flow for the Bahadurabad and the Pandu gauges. It is therefore likely that the broad peak in river flow is related to the broad peak in snowfall and subsequent snowmelt. The Pandu gauge is also one of only two gauges where the modelled river flow is less than the observations for at least part of the year, the other being the Devghat gauge on the Narayani river (Fig. 6, 4th row, left column); both of these gauges are located in the Himalayan foothills close to the region of simulated maximum total precipitation. If the simulations put the location of this maximum below these gauges this could cause the river flows at the gauges to be lower than observed. The river flow on the main trunk of the Ganges at the Farakka barrage (shown in Fig. 6, 5th row, left column), is a reasonable approximation to the observations in terms of magnitude, however the timing of the peak flow seems to be later in the models. It could be argued this also happens in some of the other gauges although it is more noticeable for the Farakka barrage. All the gauges shown here are for glacierized river basins and although snow fields and therefore snow melt are represented and the models will replicate some aspects of melt affecting river flow, glacial melt is not explicitly represented in the RCM used for these simulations; this could be important for the timing and magnitude of the maximum and minimum river flows for these catchments.

3.3 Future river flows

This section considers the future simulations from the RCM in terms of both precipitation and river flows to establish any implications for future water resources. The future annual means of both total precipitation (for the two main basins covering the gauges in this analysis) and river flows (for each gauge) are shown in Figs. 3 and 5 respectively. In both Figs. 3 and 5 the annual average is shown for the two model simulations (red line-HadCM3 and blue line-ECHAM5) by the unsmoothed (paler) lines; the smoothed (darker) lines aim to highlight any trends in the data that might be masked by the high variability shown in the annual mean of the future projections of both precipitation and river flow.

Figure 3 also highlights the variability in the future projections of total precipitation for South Asia between basins; in these simulations the Ganges/Brahmaputra catchment shows an increasing trend in total precipitation and more variation between the simulations (Fig. 3, right) than the Indus basin (Fig. 3, left), which has a much flatter trajectory to 2100.

The trends shown by the smoothed (darker) lines overlaid on top of the annual mean river flows shown in Fig. 5 highlight an upward trend in river flows at some of the gauges, in particular, the Narayani-Devghat (Fig. 5, 4th row, left column), Arun-Turkeghat (Fig. 5, 4th row, right column) and Ganges-Farakka (Fig. 5, 5th row, left column) all show an upward trend toward the 2100s that actually represents a doubling of the river flow rate which could be important for water resources for the region.

In the following analysis in Sects. 3.3.1 and 3.3.3 we focus on the modelled river flow for two future periods; 2040–2070 (referred to as 2050s) and 2068–2098 (referred to as 2080s). In Sect. 3.3.1 we consider the mean seasonal river flow for the two periods, to establish if there are changes in the seasonality of river flows in the future before focussing on the upper and lower 10 % of the river flows for the two future periods in Sect. 3.3.3. Section 3.3.4 continues to focus on the highest and lowest flows but uses the 10th and 90th percentile for each decade to compare models for each gauge.

3.3.1 Climatology analysis

The seasonal cycle of modelled river flows at each of the river gauge locations are shown in Fig. 7 for two future periods; 2050s (solid lines) and 2080s (dashed lines) for the two ensemble members (HadCM3 – red lines, ECHAM5 – blue lines). The shaded part of the plot represents the present day natural variability using the 1.5 SD of the 1971–2000 period from each model. South Asia is a very variable region, yet these models suggest the future mean river flow could lie outside the present day variability for peak flows for some of the gauges in this study; this could have important implications for water resources for the region. The gauges that show an increase in maximum river flows in Fig. 7 are mainly those in the middle of the Himalayan arc as shown in Fig. 1 with the western most (Indus gauges) and the eastern most (Brahmaputra gauges) typically still within the range of present day variability. This could be due to the changes in the influence on river flow from west to east becoming more influenced by the ASM and less by western disturbances, with basins in the centre of the Himalayas and to the north influenced by both phenomena. Figure 7 also suggests that the maximum river flows still occur mainly during the ASM for many of the gauges shown. As mentioned in Sect. 3.2 glacial melt is not explicitly represented in the RCM used for these simulations and this could have implications for the timing and magnitude of the future high and low river flows for these catchments.

Analysis of the 30 year mean is useful for understanding the general climatology of the region but often the mean does not provide the complete picture particularly when it is the periods of high and low river flow that are critical in terms of water resources. Mathison et al. (2013) highlight the importance of potential changes in the seasonal maximum and minimum river flows for the agricultural sector. The analysis in Sect. 3.3.2 considers the distribution of river flows across the region using the same river gauges and also considers changes in the upper and lower parts of the distribution of river flow.

3.3.2 High and low flow analysis

The distributions of the river flows for each of the gauges are shown in the form of probability density functions (pdfs), calculated using Kernal Density Estimation (KDE, Scott, 2009; Silverman, 1986) in Fig. 8. Figure 8 illustrates how the lowest flows dominate the distribution. In most of the gauges and both models the 1971–2000 period has the highest frequency of the lowest flows, the curves then tend to flatten in the middle of the distribution before tailing off toward zero for the frequency of the highest flows.

The Yangcun gauge on the Brahmaputra (Fig. 8, 6th row, left column) shows the least change of all the gauges between the 1971–2000 period, future periods and models, however the the distributions for the gauges downstream of Yangcun; the Pandu (Fig. 8, 6th row, right column) and the Bahadurabad (Fig. 8, 5th row, right column) are notable for their differences. The Pandu and Bahadurabad gauges have two distinct peaks in frequency, one toward the lower end of the river flow distribution, consistent with the other gauges shown, and another in the middle of the distribution, where the distribution for most other gauges flattens out. This is consistent with the broader peak in the seasonal cycle shown for these gauges in Fig. 7 and could be explained by snowmelt (see Sect. 3.2). In some of the other gauges this peak in the middle of the range of river flows is evident to a much lesser degree but tends to be restricted to the two future periods and is not evident in the present day distribution e.g. the two Karnali river gauges (Fig. 8, 3rd row). For the two future periods there is a similar shape to the distributions for each of the river gauges compared to the 1971–2000, however there is a tendancy for a reduction in the frequency of the lowest flows and an increase in the magnitude of the highest flows for both models across the gauges.

In the analysis that follows, the changes in the lowest and highest 10 % of flows are considered in more detail using two alternative approaches; one comparing the 10th and 90th percentile for each model for each decade and the other takes the relevant percentiles for the 1971–2000 period and uses these as thresholds for the two future periods.

3.3.3 Threshold analysis

In the pdfs shown in Fig. 8, the individual distributions for the gauges shown suggest that the occurrance of the lowest flows is reducing and the magnitudes of the higher flows are increasing toward the end of the century. This analysis aims to confirm this pattern by comparing the two future periods (2050s and 2080s) against the 1971–2000 period explicitly using thresholds defined by the 10th and 90th percentiles for this present day period for each river gauge. Graphical examples from the results of this analysis are shown for the Farakka Barrage on the River Ganges in Fig. 9, which shows the number of times river flows are less than the (1971–2000) 10th percentile and Fig. 10, which shows the number of times river flows are greater than the (1971–2000) 90th percentile. Each of the plots in Figs. 9 and 10 show a different decade; historical (top), 2050s (middle) and 2080s (bottom). In Fig. 9 the number of times the model is below the 1971–2000 threshold reduces in each of the future decades and in Fig. 10 the number of points increases in each of the future decades. Table 2 summarises the main results for each of the gauges from this analysis by providing the percentage change in the number of times the model simulations is less than the 10th or greater than the 90th percentile for the 1971–2000 thresholds. Table 2 illustrates that the patterns shown in Figs. 9 and 10 are generally true for almost every other gauge in the analysis. The Tehri Dam (Bhagirathi) is the only exception of the gauges shown in Table 2, showing an increase of 12 % in the number of incidences where the river flow is less than the 1971–2000 10th percentile for the 2080s; this is mainly due to the ECHAM5 model which has a high number of incidences. The Yangcun gauge (Brahmaputra) is the only gauge where there is no change in the number of incidences where the river flow is less than the 10th percentile for 1971–2000 in either the 2050s or the 2080s, probably because the lowest river flows are already very low at this gauge.

In every gauge there is an increase in the number of incidences where river flows are greater than the 90th percentile for 1971–2000 in the 2050s and 2080s in these model runs, with several of the gauges suggesting increases in the number of events above the 90th percentile for the 1971–2000 period of more than 100 %. This confirms the conclusions drawn visually from Fig. 8 that both low and high flows appear to increase in these model runs for these gauges while allowing these changes to be quantified.

3.3.4 Decadal percentile analysis

The annual timeseries shown in Fig. 5 is very variable and systematic changes throughout the century could be masked by this variability therefore in this section the 10th and 90th percentiles for each decade and each model run are considered to see if there is any systematic change on a decadal basis through to 2100. There is little difference between the two models for the 10th percentile (not shown) for most of the gauges, this is mainly due to the very low river flows at the lowest flow times of the year. Only the Pandu and Bahadurabad gauges on the Brahmaputra and the Farakka gauge on the Ganges show a non-zero value for the lowest 10 % of river flows through to the 2100s. These three gauges indicate a slight increase for the 10th percentile for each decade through to 2100.

Figure 11 shows the 90th percentile for both models calculated for each decade from 1970 to 2100 for each of the river gauges specified in Table 1. The 90th percentile values (Fig. 11) are generally much more variable than those for the 10th percentile, particularly in terms of changes through to the 2100s. Considering the gauges according to their location across the Himalayan arc from west to east, the HadCM3 simulation projects an increase in the flow for the two gauges on the Indus (Attock and Kotri gauges, shown in Fig. 11, 1st row) and the Chenab-Panjnad gauge (Fig. 11, 2nd row, left column), however ECHAM5 is generally indicating a much flatter trajectory or decreasing river flow on these rivers.

The gauges located toward the middle of the Himalayan arc in this analysis; namely Bhagirathi-Tehri (Fig. 11, 2nd row, right column), Karnali river gauges – Benighat and Chisapani (Fig. 11, 3rd row), Narayani-Devghat and Arun-Turkeghat (Fig. 11, 4th row) generally show increases across the decades to 2100 in both models. There is very close agreement between the two simulations for the Narayani-Devghat, Arun-Turkeghat (Fig. 11, 4th row) and Bhagirathi-Tehri (Fig. 11, 2nd row, right column) gauges with the former two showing less variability between decades than the others in the analysis. The Karnali-Benighat gauge (Fig. 11, 3rd row, left column) also has less variability between the decades, however there is a systematic difference between the two simulations that remains fairly constant across the decades. The Karnali-Chisapani gauge (Fig. 11, 3rd row, right column) has the largest variability between simulations and decades of the models in the analysis that are most central on the Himalayan arc, this gauge still shows an increase overall in both models although the gradient of this increase is smaller for ECHAM5 than HadCM3.

The Farakka-Ganges gauge (Fig. 11, 5th row, left column) and the Brahmaputra gauges – Bahadurabad and Pandu (Fig. 11,5th row, right column and 6th row, right column, respectively), represent the most easterly river gauges in the analysis; these gauges show an increase in both simulations through to the 2100s, although this is more pronounced in ECHAM5 than HadCM3 for the Brahmaputra gauges. There is much closer agreement between the two simulations at the Farakka-Ganges gauge (Fig. 11, 5th row, left column) which is located slightly further west than the two Brahmaputra gauges.

This analysis suggests that neither simulation is consistently showing a systematic increase in the 90th percentile of river flows across all the gauges, however it does highlight the different behaviour in the two simulations across the Himalayas. The HadCM3 simulation shows increases in western river flows which are not evident in the ECHAM5 simulation; this may be explained by the HadCM3 simulation depicting an increase in the occurance of western disturbances and an increase in total snowfall which is not evident in the ECHAM5 simulation (Ridley et al., 2013). In contrast, for the eastern gauges, both simulations show an increase in river flow, although the ECHAM5 simulation shows larger increases than HadCM3. The central gauges suggested a more mixed result, with the models more in agreement with each other; this may be due to the reducing influence of the western disturbances in the HadCM3 simulation from west to east across the Himalaya therefore resulting in smaller differences between the the two simulations at these gauges.

4 Implications of changes in future river flows

In this section we consider the implications of the projected future changes in river flows for South Asia on water resources, the key points from this discussion are summarised in Table 3. In the present day water resources in South Asia are complicated, precariously balanced between receiving some of the largest volumes of precipitation in the world and therefore the frequent risk of flooding and yet regularly enduring water shortages. The complexity is increased by the competition between states and countries for resources from rivers that flow large distances crossing state and country borders each with their own demands on resource. Annually India receives about 4000 km^3 of precipitation with 3000 km^3 falling during the ASM period. A proportion, estimated to be just over 45 % of this precipitation (approximately 1869 km^3), finds its way into the river and replenishable groundwater system (Gupta and Deshpande, 2004) which form the basis for the water resources of the country. Of the water that actually finds its way into the system only 60 % of it is currently put to beneficial use, in terms of volume; this is approximately 690 km^3 of surface water and 433 km^3 of ground water (Aggarwal et al., 2012). This means there is a gap between the amount of water resource flowing through South Asia and the actual useable amount, for example the total flow for the Brahmaputra basin is approximately 629 km^3 of which only 24 km^3 is usable (Kumar et al., 2005). There is therefore huge potential for improvements in the efficiency of systems for irrigation and the domestic water supply that could ease some of the pressures on water resources currently experienced already and predicted in the future for some areas as the demand for water increases.

In the last 50 years there have already been efficiency improvements, such as development of irrigation systems and use of high yielding crop varieties that have fuelled the rapid development in agriculture across South Asia making the region more self-sustained and alleviating poverty (Kumar et al., 2005); however this has had a large impact on the regions river ecosystems resulting in habitat loss and reduced biodiversity (Sarkar et al., 2012). Vörösmarty et al. (2010) find that in developing regions, where investment in water infrastructure is low and water security is threatened there tends to be a coincident risk of biodiversity loss, with the main threat due to water resource development and increased pollution from the use of pesticides and fertilizer. Gupta and Deshpande (2004) estimate that a minimum storage of 385 km^3 is needed across all the basins in India to balance seasonal flows and irrigate 760 000 km^2

although how this translates to an individual river in terms of the river flows needed to maintain ecosystems and biodiversity (also referred to as environmental flows) is a complex problem. Historically arbitrary thresholds based on a percentage of the annual mean flow have been used to estimate minimum flows, but these simplistic estimates do not take account of the flow variability that is crucial for sustaining river ecosystems (Arthington et al., 2006; Smakhtin et al., 2006). Environmental flows are defined by Smakhtin and Anputhas (2006) as the ecologically acceptable flow regime designed to maintain a river in an agreed or predetermined state. The variability in river flows through the year have important ecological significance; for example low flows are important for algae control and therefore maintaining water quality, while high flows are important for wetland flooding and preserving the river channel. When considering the implications of future changes in climate on river flows and therefore surface water resources, an estimate of the environmental requirement, both in terms of the flow variability as well as the minimum flows, are an important consideration. These important ecological thresholds together with the flows which cause inundation and crop damage have been calculated for individual basins, such as the lower Brahmaputra river basin by Gain et al. (2013) and the East Rapti River in Nepal by Smakhtin et al. (2006), however they are not easily quantified in general terms for different rivers with many methods requiring calibration for applications to different regions.

In India the domestic requirement for water is the highest priority but is only 5 % of the total demand (this equates to approximately 30 km^3 of which 17 km^3 is from surface water and the rest groundwater). Irrigation is the second highest priority accounting for a much greater proportion, approximately 80 % of India's total demand for water; this equates to more than 520 km^3 with 320 km^3 from surface water and 206 km^3 from groundwater (Kumar et al., 2005). Biemans et al. (2013) study future water resources for food production using LPJml and the HNRCMS. The LPJmI simulated extraction varies considerably between basins; the largest occuring in the Indus (343 $\text{km}^3\,\text{year}^{-1}$) followed by the Ganges (281 $\text{km}^3\,\text{year}^{-1}$) and Brahmaputra (45 $\text{km}^3\,\text{year}^{-1}$). The

Brahmaputra has the smallest percentage of irrigated crop production (approximately 40 %) followed by the Ganges (less than 75 %) and the Indus where more than 90 % of crop production is on irrigated land. The Indus has the largest proportion of water sourced from rivers and lakes of the three basins. LPJml also simulates ground water extractions Biemans et al. (2013) these are thought to be important for the Indus and parts of the Ganges but not the Brahmaputra. The model simulations presented in this analysis do not explicitly include groundwater, primarily focusing on river flows and therefore the surface water component of resource for this region. There is also no irrigation included in these simulations, which could be important particularly on the basin scale. The impacts of extensive irrigation on the atmosphere are complex but could have a positive impact on water availability (Harding et al., 2013) due to evaporation and water being recycled within the basin, for example, Tuinenburg et al. (2014) estimate that up to 35 % of additional evaporation is recycled within the Ganges basin.

In general the analysis here shows that the magnitudes of the higher river flows could increase for these gauges (see Table 1), in some cases these increases are above the range of variability used for this analysis (1.5 SD). While this could be positive in terms of surface water resources for irrigation, the potential changes seem to occur during the ASM season and therefore when river flow is at its maximum; therefore this increase may not be critical for water resources but could still be beneficial where there is the capacity to store the additional flow for use during periods of low flow. Additional water storage capacity for example through rainwater harvesting, could greatly increase the useable water resource for the Ganges–Brahmaputra catchments (Kumar et al., 2005) and potentially alleviate the increased risk of flooding during the ASM when rainfall is most persistent and rivers are already at their peak flow. South Asia, even in the current climate, is particularly susceptible to flooding due to the high temporal and spatial variability of rainfall of the region, for example approximately 20 % of Bangladesh floods annually (Mirza, 2002). Several studies have highlighted increases in both the extremes (Sharma, 2012; Rajeevan et al., 2008; Goswami et al., 2006; Joshi and Rajeevan,

2006) and the variability (Gupta et al., 2005) of precipitation in recent years, where extreme rainfall events have resulted in catastrophic levels of river flooding. Over 30 million people in India alone are affected by floods and more than 1500 lives are lost each year (Gupta et al., 2003), the economic cost of flooding is also considerable with the cumulative flood related losses estimated to be of the order of USD 16 billion between 1978 and 2006 (Singh and Kumar, 2013).

The timing of the peak flows of major rivers in this region is also very important in terms of flooding. In 1998 the peak flows of the Ganges and the Brahmaputra rivers occurred within 2 days of each other resulting in devastating flooding across the entire central region of Bangladesh inundating aproximately 70 % of the country, the flood waters then remained above danger levels for more than 60 days (Mirza, 2002). This event caused extensive loss of life and livelihood in terms of damaged crops, fisheries and property with the slow recedance of flood waters hindering the relief operation and recovery of the region. This analysis does not suggest any change to the timing of the peak flows, only the magnitude, however given the high probability of two rivers in this region having coincident peak flows in any given year (Mirza, 2002) and the likelihood that severe flooding will result, means that an increase in the magnitude of the peak could still be significant. Flooding can have a large impact on crops, for example in Bangladesh over 30 % of the total flood related damages are due to the loss of crops; the estimated crop damage from the 1998 floods was estimated to be 3.0 million t (Gain et al., 2013). Slow receeding of flood water can also mean the ground is not in a suitable condition to sow the next crop, restricting the growing time and potentially affecting crop yields for the following year.

Another proposed though controversial method aimed at alleviating flooding in the South Asia region is inter-basin transfer through the National River Linking Project (NRLP); this is an attempt to redistribute the water between rivers by linking those rivers with a surplus to those with a deficit (Gupta and Deshpande, 2004). The success of these projects depends on the elevation of the catchment providing the water being above that of the receiving catchment so catchments with a low elevation such as the Brahmaputra can only transfer a small amount despite having large problems with flooding. On the other hand a limited amount of flooding could also be a benefit, particularly for rice crops, as the inundation of clear water benefits crop yield due to the fertilization effect of nitrogen producing blue-green algae in the water (Mirza et al., 2003).

In these simulations the occurrance of the lowest flows potentially reduces in the future, which could translate into an increase in the surface water resource in this region, for periods when the river flows are traditionally very low and water is usually scarce. This could mean that the current and increasing pressure on ground water (Rodell et al., 2009) may be alleviated in future years. Alternatively increases in the lowest flows may enable adaptation to a changing climate and the modification of irrigation practises. Current projections of future climate suggest that temperatures could also increase for this region (Cruz et al., 2007), this poses a threat to crop yields of a different kind because this is a region where temperatures are already at a physiological maxima for some crops (Gornall et al., 2010). Rice yield, for example, is adversely affected by temperatures above 35 °C at the critical flowering stage of its development (Yoshida, 1981) and wheat yields could be also affected by rising temperatures, with estimated losses of 4–5 million t $(^{\circ}\mathrm{C})^{-1}$ temperature rise through the growing period (Aggarwal et al., 2012). Additional water resource for irrigation at previously low flow times of the year could allow sowing to take place at a different time of the year in order to avoid the highest temperatures, thereby reducing the likelihood of crop failure. However with increasing variability and extremes, a potential feature of the future climate for this region, there is also the increased risk of longer periods with below average rainfall and potentially more incidences of drought; this could lead to additional demand for water for irrigation to prevent crops becoming water stressed (Aggarwal et al., 2012). There may also be increases in demand from other sources other than agriculture, for example the increasing population (United Nations, 2013) or the reduced availability of ground water of an acceptable quality for domestic use (Gregory et al., 2005). Any of these factors, either individually or combined, could effectively cancel out any or all increases in resource from increased river flow due to climate change.

5 Conclusions

In this analysis the first 25 km resolution regional climate projections of riverflow for the South Asia region are presented. A sub-selection of the HNRCMs are used to provide runoff to a river routing model in order to provide river flow rate which can be compared directly with a downscaled ERAint simulation and any available observation data for river basins in the South Asia region. This analysis focuses on the major South Asia river basins which originate in the glaciated Hindu-Kush Karakoram Himalaya; Ganges/Brahmaputra and the Indus. The aim of this analysis is two-fold; firstly to understand the river flows in the RCM in the two simulations and how useful they are for understanding the changes in water resources for South Asia and secondly to understand what the projected changes in river flow to the 2100s might mean for water resources across the Himalaya region.

The two simulations in this analysis cannot capture the full range of variability, however the two GCMs that are downscaled using this RCM do capture a range of temperatures and variability in precipitation similar to the AR4 ensemble for Asia (Christensen et al., 2007) which is for a much larger domain than the HighNoon domain analysed here (Mathison et al., 2013). A number of GRDC gauge stations (GRDC, 2014), selected to capture the range of conditions across the Himalayan arc and sample the major river basins, provide the observations of river flow for comparison against the simulations. The lack of recent river flow data limited the gauges that could be selected for analysis, however using the downscaled ERAint simulation provides a constrained estimate of the South Asia water cycle in the absence of robust observations and is used in addition to the observations to provide a useful benchmark against which to compare the downscaled GCM simulations. In general there is a tendancy for overestimation of river flow rate across the selected gauges compared to the GRDC observations, however comparison against the ERAint simulation is more mixed with some gauges showing higher and others lower river flows for the downscaled GCMs compared with ERAint. However in general most of the simulations broadly agree with observations and ERAint to within the range of natural variability (chosen to be 1.5 SD for this analysis) and agree on the periods of highest and lowest river flow, indicating that the RCM is able to capture the main features of both the climate and hydrology of the region.

The simulations suggest that the annual average river flow is increasing toward the 2100s, although these trends are often masked by the large inter-annual variability of river flows in this region, for some of the gauges the river flow rates are almost doubled by the end of the century. These increases in river flows are reflected in the seasonal cycle for the two future periods (2050s and 2080s) which indicate that most of the changes occur during peak flow periods with some gauges showing changes above the range of present day natural variability. These gauges tend to be toward the middle of the Himalayan arc, so this could be due to the increasing influence of the ASM and reducing influence of western disturbances from west to east. The gauges located furthest west and east in this analysis seem to lie within the present day natural variability. The analysis shown here does not suggest a systematic change in the models for the timing of the maximum and minimum river flows relative to the present day suggesting an over all increase in water resources at the top and bottom of the distribution. This has positive and negative implications with potentially more resource during usually water scarce periods but also carries implications for an already vulnerable population in terms of increased future flood risk during periods where the river flow is particularly high. Bangladesh is particularly susceptible to flooding, therefore any increase in maximum flows for rivers in this region could be important in terms of loss of life, livelihoods, particularly agriculture and damage to infrastructure. Historically management policies for rivers in this region have focussed on percentage of the average annual flow which does not take into account the importance of flow variability as well as minimum flows, which are important for sustaining river ecosystems.

While this analysis suggests a general increase in potential water resources from rivers for this region to 2100 due to climate change, there are a number of factors which could have a larger effect on water resources for this region and effectively cancel out any increase. For example rising population, depletion of ground water, increases in demand for water from sources other than agriculture. In addition increasing variability of the South Asia climate could lead to long periods with below average rainfall which could also increase the demand for irrigation. Further more the results shown here do not currently explicitly include the glacial contribution to river flow for these catchments and gauges. Including glacial processes in the form of a glacier model together with river routing within the land-surface representation will be useful to establish if the contribution from glaciers changes the timing and/or magnitude of both the lowest and highest flows in these gauges. Likewise including representation of water extraction (both from rivers and groundwater) particularly for irrigation, the biggest user of water in the region, will help to provide a more complete picture of the water resources for the South Asia region. Understanding the interactions between availability of water resources, irrigation and food production for this region by using a more integrated approach, such as that used in Biemans et al. (2013) may also help with understanding how pressures on resources could change with time. In support of this work and others, there is also a need for good quality observations of both precipitation and river flow that is available for long enough time periods to conduct robust water resource assessments for this region.

Acknowledgements. The research leading to these results has received funding from the European Union Seventh Framework Programme FP7/2007-2013 under grant agreement no 603864. Camilla Mathison, Pete Falloon and Andy Wiltshire were supported by the Joint UK DECC/Defra Met Office Hadley Centre Climate Programme (GA01101). Thanks to Neil Kaye for his GIS expertise.

References

Aggarwal, P., Talukdar, K., and Mall, R.: Potential Yields of Rice-Wheat System in the Indo-Gangetic Plains of India, Rice-Wheat Consortium for the Indo-Gangetic Plains, New Delhi, India, Rice-Wheat Consortium Paper Series, 10, 16, 2000. 5793

Aggarwal, P., Palanisami, K., Khanna, M., and Kakumanu, K.: Climate change and food security of India: adaptation strategies for the irrigation sector, World Agr., 3, 20–26, 2012. 5792, 5811, 5815

Akhtar, M., Ahmad, N., and Booij, M.: The impact of climate change on the water resources of Hindukush–Karakorum–Himalaya region under different glacier coverage scenarios, J. Hydrol., 355, 148–163, doi:10.1016/j.jhydrol.2008.03.015, 2008. 5793

Andermann, C., Bonnet, S., and Gloaguen, R.: Evaluation of precipitation data sets along the Himalayan front, Geochem. Geophy. Geosy., 12, Q07023, doi:10.1029/2011GC003513, 2011. 5795

Annamalai, H., Hamilton, K., and Sperber, K.: The South Asian summer monsoon and its relationship with ENSO in the IPCC AR4 simulations, J. Climate, 20, 1071–1092, doi:10.1175/JCLI4035.1, 2007. 5793, 5797

Arthington, A. H., Bunn, S. E., Poff, N. L., and Naiman, R. J.: The challenge of providing environmental flow rules to sustain river ecosystems, Ecol. Appl., 16, 1311–1318, doi:10.1890/1051-0761(2006)016[1311:TCOPEF]2.0.CO;2, 2006. 5812

Bajracharya, S. and Shrestha, B.: The Status of Glaciers in the Hindu Kush-Himalayan Region, Kathmandu: ICIMOD, available at: http://lib.icimod.org/record/9419, last access: November 2014, 2011. 5796

Barnett, T., Adam, J., and Lettenmaier, D.: Potential impacts of a warming climate on water availability in snow-dominated regions, Nature, 438, 303–309, doi:10.1038/nature04141, 2005. 5792

Biemans, H., Speelman, L., Ludwig, F., Moors, E., Wiltshire, A., Kumar, P., Gerten, D., and Kabat, P.: Future water resources for food production in five South Asian river basins and potential for adaptation – a modeling study, Sci. Total Environ., 468–469, S117–S131, doi:10.1016/j.scitotenv.2013.05.092, 2013. 5799, 5803, 5812, 5813, 5818

Christensen, J., Hewitson, B., Busuioc, A., Chen, A., Gao, X., Held, I., Jones, R., Kolli, R., Kwon, W.-T., Laprise, R., na Rueda, V. M., Mearns, L., Meneńdez, C., Räisänen, J., Rinke, A., Sarr, A., and Whetton, P.: Regional climate projections, in: Climate Change 2007: the

Physical Science Basis. Contribution of Working Group I, Fourth Assessment Report of the Intergovernmental Panel on Climate Change, available at: https://www.ipcc.ch/publications_and_data/ar4/wg1/en/ch11.html, last access: October 2014, 2007. 5792, 5797, 5800, 5816

Clark, D. B. and Gedney, N.: Representing the effects of subgrid variability of soil moisture on runoff generation in a land surface model, J. Geophys. Res., 113, D10111, doi:10.1029/2007JD008940, 2008. 5798

Collins, D. N., Davenport, J. L., and Stoffel, M.: Climatic variation and runoff from partially-glacierised Himalayan tributary basins of the Ganges, Sci. Total Environ., 468–469, S48–S59, doi:10.1016/j.scitotenv.2013.10.126, 2013. 5794

Cruz, R., Harasawa, H., Lal, M., Wu, S., Anokhin, Y., Punsalmaa, B., Honda, Y., Jafari, M., Li, C., and Huu Ninh, N.: Asia. Climate change 2007: impacts, adaptation and vulnerability, in: Contribution of Working Group II, Fourth Assessment Report of the Intergovernmental Panel on Climate Change, 469–506, available at: https://www.ipcc.ch/publications_and_data/ar4/wg2/en/ch10.html, last access: October 2014, 2007. 5815

Dhar, O. and Nandargi, S.: A study of floods in the Brahmaputra basin in India, Int. J. Climatol., 20, 771–781, doi:10.1002/1097-0088(20000615)20:7<771::AID-JOC518>3.0.CO;2-Z, 2000. 5796

Dimri, A., Yasunari, T., Wiltshire, A., Kumar, P., Mathison, C., Ridley, J., and Jacob, D.: Application of regional climate models to the Indian winter monsoon over the western Himalayas, Sci. Total Environ., 468, S36–S47, 2013. 5794

Dolman, A. J. and Gregory, D.: The parametrization of rainfall interception in GCMs, Q. J. Roy. Meteor. Soc., 118, 455–467, doi:10.1002/qj.49711850504, 1992. 5798

Essery, R. L. H., Best, M. J., and Cox, P. M.: MOSES 2.2 technical documentation, Hadley Centre Technical Note, 30, available at: http://www.metoffice.gov.uk/archive/hadley-centre-technical-note-30, last access: February 2015, 2001. 5798

Essery, R. L. H., Best, M. J., Betts, R. A., Cox, P. M., and Taylor, C.: Explicit representation of subgrid heterogeneity in a GCM land surface scheme, J. Hydrometeorol., 4, 530–543, doi:10.1175/1525-7541(2003)004<0530:EROSHI>2.0.CO;2, 2003. 5797, 5798

Falloon, P., Betts, R., and Bunton, C.: New global river routing scheme in the unified model, Hadley Centre Technical Note, 72, available at: http://www.metoffice.gov.uk/archive/hadley-centre-technical-note-72, last access: February 2015, 2007. 5799

Falloon, P., Betts, R. A., Wiltshire, A., Dankers, R., Mathison, C., McNeall, D., Bates, P., and Trigg, M.: Validation of river flows in hadgem1 and hadcm3 with the trip river flow model, J. Hydrometeorol., 12, 1157–1180, doi:10.1175/2011JHM1388.1, 2011. 5793, 5803

Fekete, B. M., Vörösmarty, C. J., and Lammers, R. B.: Scaling gridded river networks for macroscale hydrology: development, analysis, and control of error, Water Resour. Res., 37, 1955–1967, doi:10.1029/2001WR900024, 2001. 5798

Fujita, K. and Nuimura, T.: Spatially heterogeneous wastage of Himalayan glaciers, P. Natl. Acad. Sci. USA, 108, 14011–14014, 2011. 5792

Gain, A. K., Apel, H., Renaud, F. G., and Giupponi, C.: Thresholds of hydrologic flow regime of a river and investigation of climate change impact the case of the Lower Brahmaputra river Basin, Climatic Change, 120, 463–475, doi:10.1007/s10584-013-0800-x, 2013. 5812, 5814

Gedney, N. and Cox, P.: The sensitivity of global climate model simulations to the representation of soil moisture heterogeneity, J. Hydrometeorol., 4, 1265–1275, doi:10.1175/1525-7541(2003)004<1265:TSOGCM>2.0.CO;2, 2003. 5798

Gordon, C., Cooper, C., Senior, C. A., Banks, H., Gregory, J. M., Johns, T. C., Mitchell, J. F. B., and Wood, R. A.: The simulation of SST, sea ice extents and ocean heat transports in a version of the Hadley Centre coupled model without flux adjustments, Clim. Dynam., 16, 147–168, doi:10.1007/s003820050010, 2000. 5797

Gornall, J., Betts, R., Burke, E., Clark, R., Camp, J., Willett, K., and Wiltshire, A.: Implications of climate change for agricultural productivity in the early twenty-first century, Philos. T. Roy. Soc. B, 365, 2973–2989, doi:10.1098/rstb.2010.0158, 2010. 5815

Goswami, B. and Xavier, P. K.: Dynamics of "internal" interannual variability of the Indian summer monsoon in a GCM, J. Geophys. Res., 110, D24104, doi:10.1029/2005JD006042, 2005. 5792, 5800

Goswami, B. N., Venugopal, V., Sengupta, D., Madhusoodanan, M. S., and Xavier, P. K.: Increasing trend of extreme rain events over India in a warming environment, Science, 314, 1442–1445, doi:10.1126/science.1132027, 2006. 5813

GRDC: The Global Runoff Data Centre, 56002 Koblenz, Germany, 2014. 5794, 5795, 5802, 5816

Gregory, P., Ingram, J., and Brklacich, M.: Climate change and food security, Philos. T. R. Soc. B, 360, 2139–2148, doi:10.1098/rstb.2005.1745, 2005. 5792, 5815

Gupta, A. D., Babel, M. S., Albert, X., and Mark, O.: Water sector of Bangladesh in the context of integrated water resources management: a review, Int. J. Water Resour. D., 21, 385–398, doi:10.1080/07900620500037818, 2005. 5814

Gupta, S. and Deshpande, D.: Water for India in 2050: first order assessment of available options, Curr. Sci. India, 86, 1216–1224, 2004. 5792, 5811, 5814

Gupta, S., Javed, A., and Datt, D.: Economics of flood protection in India, Nat. Hazards, 28, 199–210, 2003. 5814, 5829

Harding, R., Blyth, E., Tuinenburg, O., and Wiltshire, A.: Land atmosphere feedbacks and their role in the water resources of the Ganges basin, Sci. Total Environ., 468–469, S85–S92, doi:10.1016/j.scitotenv.2013.03.016, 2013. 5796, 5799, 5813

Immerzeel, W., van Beek, L., and Bierkens, M.: Climate change will affect the Asian water towers, Science, 328, 1382–1385, doi:10.1126/science.1183188, 2010. 5792

Johnston, R. and Smakhtin, V.: Hydrological Modeling of Large river Basins: How Much is Enough?, Water Resour. Manag., 28, 2695–2730, doi:10.1007/s11269-014-0637-8, 2014. 5795

Jones, R. G., Noguer, M., Hassell, D. C., Hudson, D., Wilson, S. S., Jenkins, G. J., and Mitchell, J. F.: Generating high resolution climate change scenarios using PRECIS, Met Office Hadley Centre, Exeter, UK, 0–40, available at: http://www.metoffice.gov.uk/media/pdf/6/5/PRECIS_Handbook.pdf, last access: February 2015, 2004. 5797

Joshi, U. and Rajeevan, M.: Trends in precipitation extremes over India, National Climate Centre Research report, 3, available at: http://www.imdpune.gov.in/ncc_rept/RESEARCH%20%20REPORT%203.pdf, last access: February 2015, 2006. 5813

Kapnick, S. B., Delworth, T. L., Ashfaq, M., Malyshev, S., and Milly, P. C. D.: Snowfall less sensitive to warming in Karakoram than in Himalayas due to a unique seasonal cycle, Nat. Geosci., 7, 834–840, doi:10.1038/ngeo2269, 2014. 5794

Kumar, P., Wiltshire, A., Mathison, C., Asharaf, S., Ahrens, B., Lucas-Picher, P., Christensen, J. H., Gobiet, A., Saeed, F., Hagemann, S., and Jacob, D.: Downscaled climate change projections with uncertainty assessment over India using a high resolution multi-model approach, Sci. Total Environ., 468–469, S18–S30, doi:10.1016/j.scitotenv.2013.01.051, 2013. 5797, 5799, 5800

Kumar, R., Singh, R., and Sharma, K.: Water resources of India, Curr. Sci. India, 89, 794–811, 2005. 5792, 5811, 5812, 5813

Linsley, R., Kohler, M., and Paulhus, J.: Hydrology for Engineers, McGraw-Hill series in water resources and environmental engineering, McGraw-Hill, available at: http://books.google.co.uk/books?id=9vROAAAAMAAJ, last access: February 2015, 1982. 5798

Lucas-Picher, P., Christensen, J. H., Saeed, F., Kumar, P., Asharaf, S., Ahrens, B., Wiltshire, A. J., Jacob, D., and Hagemann, S.: Can regional climate models represent the Indian Monsoon?, J. Hydrometeorol., 12, 849–868, doi:10.1175/2011JHM1327.1, 2011. 5793, 5799

Mathison, C., Wiltshire, A., Dimri, A., Falloon, P., Jacob, D., Kumar, P., Moors, E., Ridley, J., Siderius, C., Stoffel, M., and Yasunari, T.: Regional projections of North Indian climate for adaptation studies, Sci. Total Environ., 468–469, S4–S17, doi:10.1016/j.scitotenv.2012.04.066, 2013. 5792, 5793, 5797, 5799, 5800, 5801, 5806, 5816

McMillan, H., Freer, J., Pappenberger, F., Krueger, T., and Clark, M.: Impacts of uncertain river flow data on rainfall–runoff model calibration and discharge predictions, Hydrol. Process., 24, 1270–1284, 2010. 5803

Mirza, M. M. Q.: Global warming and changes in the probability of occurrence of floods in Bangladesh and implications, Global Environmental Change, 12, 127–138, doi:10.1016/S0959-3780(02)00002-X, 2002. 5813, 5814

Mirza, M. M. Q., Warrick, R., Ericksen, N., and Kenny, G.: Trends and persistence in precipitation in the Ganges, Brahmaputra and Meghna river basins, Hydrological Sciences Journal, 43, 845–858, doi:10.1080/02626669809492182, 1998. 5795

Mirza, M. M. Q., Warrick, R. A., and Ericksen, N. J.: The Implications of Climate Change on Floods of the Ganges, Brahmaputra and Meghna Rivers in Bangladesh, Climatic Change, 57, 287–318, doi:10.1023/A:1022825915791, 2003. 5815

Moors, E. J., Groot, A., Biemans, H., van Scheltinga, C. T., Siderius, C., Stoffel, M., Huggel, C., Wiltshire, A., Mathison, C., Ridley, J., Jacob, D., Kumar, P., Bhadwal, S., Gosain, A., and Collins, D. N.: Adaptation to changing water resources in the Ganges basin, northern India, Environ. Sci. Policy, 14, 758–769, doi:10.1016/j.envsci.2011.03.005, 2011. 5797

Morse, A., Prentice, C., and Carter, T.: Assessments of climate change impacts, Ensembles: Climate change and its impacts: Summary of research and results from the ENSEMBLES project, 107–129, available at: http://ensembles-eu.metoffice.com/docs/Ensembles_final_report_Nov09.pdf, last access: February 2015, 2009. 5799

Nohara, D., Kitoh, A., Hosaka, M., and Oki, T.: Impact of climate change on river discharge projected by multimodel ensemble, J. Hydrometeorol., 7, 1076–1089, doi:10.1175/JHM531.1, 2006. 5800

Oki, T. and Sud, Y. C.: Design of Total Runoff Integrating Pathways (TRIP). A global river channel network, Earth Interact., 2, 1–37, doi:10.1175/1087-3562(1998)002<0001:DOTRIP>2.3.CO;2, 1998. 5793, 5798

Oki, T., Nishimura, T., and Dirmeyer, P.: Assessment of annual runoff from land surface models using Total Runoff Integrating Pathways (TRIP), J. Meteorol. Soc. Jpn., 77, 235–255, doi:10.1080/02626668509490989, 1999. 5799, 5803

Pope, V., Gallani, M. L., Rowntree, P. R., and Stratton, R. A.: The impact of new physical parametrizations in the Hadley Centre climate model: HadAM3, Clim. Dynam., 16, 123–146, doi:10.1007/s003820050009, 2000. 5797

Rajeevan, M., Bhate, J., and Jaswal, A. K.: Analysis of variability and trends of extreme rainfall events over India using 104 years of gridded daily rainfall data, Geophys. Res. Lett., 35, L18707, doi:10.1029/2008GL035143, 2008. 5813

Ridley, J., Wiltshire, A., and Mathison, C.: More frequent occurrence of westerly disturbances in Karakoram up to 2100, Sci. Total Environ., 468–469, S31–S35, doi:10.1016/j.scitotenv.2013.03.074, 2013. 5794, 5810

Rodell, M., Velicogna, I., and Famiglietti, J.: Satellite-based estimates of groundwater depletion in India, Nature, 460, 999–1002, doi:10.1038/nature08238, 2009. 5792, 5815

Roeckner, E., Bäuml, G., Bonaventura, L., Brokopf, R., Esch, M., Giorgetta, M., Hagemann, S., Kirchner, I., Kornblueh, L., Manzini, E., Rhodin, A., Schlese, U., Schulzweida, U., and Tompkins, A.: The atmospheric general circulation model ECHAM 5. PART I: Model description, Max Planck Institute for Meteorology Rep. 349, available at: http://www.mpimet.mpg.de/fileadmin/publikationen/Reports/max_scirep_349.pdf, last access: February 2015, 2003. 5797

Sarkar, U. K., Pathak, A. K., Sinha, R. K., Sivakumar, K., Pandian, A. K., Pandey, A., Dubey, V. K., and Lakra, W. S.: Freshwater fish biodiversity in the River Ganga (India): changing pattern, threats and conservation perspectives, Rev. Fish Biol. Fisher., 22, 251–272, doi:10.1007/s11160-011-9218-6, 2012. 5811

Scott, D.: Multivariate Density Estimation: Theory, Practice, and Visualization, vol. 383, mainly chapter 6, John Wiley & Sons, USA, 2009. 5806

Sharma, D.: Situation analysis of flood disaster in south and southeast Asia – a need of integrated approach, International Journal of Science, Environment and Technology, 1, 167–173, 2012. 5813

Silverman, B. W.: Density estimation for statistics and data analysis, Monographs on Statistics and Applied Probability, Chapman and Hall, London, 26, mainly chapters 3 and 4, 1986. 5806

Simmons, A., Uppala, S., Dee, D., and Kobayashi, S.: ERA-Interim: new ECMWF reanalysis products from 1989 onwards, ECMWF, Shinfield, Reading, UK, Newsletter – Winter 2006/07, 110, 0–11, 2007. 5793, 5795, 5797

Singh, O. and Kumar, M.: Flood events, fatalities and damages in India from 1978 to 2006, Nat. Hazards, 69, 1815–1834, 2013. 5814

Smakhtin, V. and Anputhas, M.: An assessment of environmental flow requirements of Indian river basins, IWMI Research Report 107, available at: http://www.iwmi.cgiar.org/Publications/IWMI_Research_Reports/PDF/PUB107/RR107.pdf, last access: October 2014, 2006. 5812

Smakhtin, V. U., Shilpakar, R. L., and Hughes, D. A.: Hydrology-based assessment of environmental flows: an example from Nepal, Hydrolog. Sci. J., 51, 207–222, doi:10.1623/hysj.51.2.207, 2006. 5812

Thenkabail, P. S., Schull, M., and Turral, H.: Ganges and Indus river basin land use/land cover LULC) and irrigated area mapping using continuous streams of MODIS data, Remote Sens. Environ., 95, 317–341, doi:10.1016/j.rse.2004.12.018, 2005. 5795

Tuinenburg, O. A., Hutjes, R. W. A., Stacke, T., Wiltshire, A., and Lucas-Picher, P.: Effects of irrigation in india on the atmospheric water budget, J. Hydrometeorol., 15, 1028–1050, doi:10.1175/JHM-D-13-078.1, 2014. 5799, 5813

United Nations: Fertility Levels and Trends as Assessed in the 2012 Revision of World Population Prospects, Department of Economic and Social Affairs, Population Division, available at: http://esa.un.org/unpd/wpp/index.htm, last access: August 2014, 2013. 5791, 5815

Vörösmarty, C., Fekete, B., Meybeck, M., and Lammers, R.: Geomorphometric attributes of the global system of rivers at 30 min spatial resolution, J. Hydrol., 237, 17–39, doi:10.1016/S0022-1694(00)00282-1, 2000a. 5798

Vörösmarty, C., Fekete, B., Meybeck, M., and Lammers, R.: Global system of rivers: its role in organizing continental land mass and defining land-to-ocean linkages, Global Biogeochem. Cy., 14, 599–621, doi:10.1029/1999GB900092, 2000b. 5798

Title Page
Abstract | Introduction
Conclusions | References
Tables | Figures
◀| |▶
◀ ▶
Back | Close
Full Screen / Esc
Printer-friendly Version
Interactive Discussion

Vörösmarty, C. J., McIntyre, P. B., Gessner, M. O., Dudgeon, D., Prusevich, A., Green, P., Glidden, S., Bunn, S. E., Sullivan, C. A., Liermann, C. R., and Davies, P. M.: Global threats to human water security and river biodiversity, Nature, 467, 555–561, doi:10.1038/nature09440, 2010. 5811

Wescoat Jr., J.: Managing the Indus River basin in light of climate change: four conceptual approaches, Global Environ. Chang., 1, 381–395, doi:10.1016/0959-3780(91)90004-D, 1991. 5795

Wiltshire, A. J.: Climate change implications for the glaciers of the Hindu Kush, Karakoram and Himalayan region, The Cryosphere, 8, 941–958, doi:10.5194/tc-8-941-2014, 2014. 5793, 5794

Yatagai, A., Kamiguchi, K., Arakawa, O., Hamada, A., Yasutomi, N., and Kitoh, A.: Aphrodite: constructing a long-term daily gridded precipitation dataset for asia based on a dense network of rain gauges., B. Am. Meteorol. Soc., 93, 1401–1415, doi:10.1175/BAMS-D-11-00122.1, 2012. 5794, 5795

Yoshida, S.: Fundamentals of rice crop science, Manila, Philipines, available at: http://books.irri.org/9711040522_content.pdf, last access: October 2014, 1981. 5815

Table 1. Table listing the rivers and gauges (including their location) used in this analysis; all the observations shown here are from GRDC. The abbreviations used in Fig. 1 are given in column one. The Years of data column includes the number of years that data is available since 1950 with c to denote where data is continuous and u to show where the data is available for that number of years but not as a continuous dataset.

Map abbreviation	River name	Gauge name	Latitude	Longitude	Years of data
IND_KOT	Indus	Kotri	25.37	68.37	14u (1950–1978)
IND_ATT	Indus	Attock	33.9	72.25	6c (1973–1979)
CHE_PAN	Chenab	Panjnad	29.35	71.03	6c (1973–1979)
BHA_TEH	Bhagirathi	Tehri Dam	30.4	78.5	3c (2001–2004)
KAR_BEN	Karnali River	Benighat	28.96	81.12	25u (1963–1993)
KAR_CHI	Karnali River	Chisapani	28.64	81.29	31c (1962–1993)
NAR_DEV	Narayani	Devghat	27.71	84.43	23u (1963–1993)
ARU_TUR	Arun	Turkeghat	27.33	87.19	10c (1976–1986)
GAN_FAR	Ganges	Farakka	25.0	87.92	18u (1950–1973)
BRA_BAH	Brahmaputra	Bahadurabad	25.18	89.67	12u (1969–1992)
BRA_YAN	Brahmaputra	Yangcun	29.28	91.88	21u (1956–1982)
BRA_PAN	Brahmaputra	Pandu	26.13	91.7	13u (1956–1979)

Title Page
Abstract | Introduction
Conclusions | References
Tables | Figures
◄ | ►
Back | Close
Full Screen / Esc
Printer-friendly Version
Interactive Discussion

Table 2. Table showing the average percentage change for the two models in the number of times the modelled river flow is less than the 10th percentile and greater than the 90th percentile of the 1970–2000 period for the 2050s and 2080s future periods.

River	Gauge	< 10th percentile % change		> 90th percentile % change	
		2050s	2080s	2050s	2080s
Indus	Kotri	−55.4	−89.2	60.8	55.4
Indus	Attock	−70.3	−95.9	70.3	81.1
Karnali River	Benighat	−39.2	−73.0	63.5	81.1
Karnali River	Chisapani	−27.0	−56.8	60.8	79.7
Narayani	Devghat	−21.6	−54.1	75.7	110.8
Arun	Turkeghat	−63.5	−90.5	66.2	116.2
Brahmaputra	Yangcun	0	0	20.3	36.5
Brahmaputra	Pandu	−59.5	−79.7	47.3	113.5
Brahmaputra	Bahadurabad	−48.6	−64.9	67.6	114.9
Ganges	Farakka	−36.5	−52.7	68.9	102.7
Bhagirathi	Tehri Dam	−4.1	**12.2**[*]	13.5	41.9
Chenab	Panjnad	−58.1	−83.8	43.2	50.0

[*] This value is the only positive value in the table.

Table 3. Table of implications of changes in water resources.

Types of change	Implications for water resource	Adaptation options	Other issues
Large annual variability	Abundance some years and scarcity in others make it difficult to plan budgets for different users.	Building storage capacity e.g. rainwater harvesting. Improvement of irrigations systems. Development of water efficient, high yielding crop varieties.	Type of water storage is important e.g. reservoirs/dams have both political and ecological implications. Developing new crops takes time.
Changes in peak flow – timing and magnitude	Increases in peak flows could be positive for irrigation and domestic supply but could increase the risk of flooding. Peak flows occurring later and/or decreases in peak flows could reduce availability of water for irrigation at crucial crop development stages negatively impacting yields.	Improving river channel capacity. Diverting excess water to a different valley. Storing the excess water for low flow periods e.g. through rainwater harvesting. Improving drainage and water recycling. Adopting varieties of crops that grow when water for irrigation is more readily available	Flood protection levels do not match demographic trends so vulnerability to flooding remains high in this region (Gupta et al., 2003). Market development for new crops takes time
Changes in low flows – timing and magnitude	Increases in the magnitude of the low flows could be positive for irrigation and domestic supply. Decreases could mean less resource available for irrigation leading to reduced yields	Adaptations to avoid flooding during peak flow periods could provide resource during low flow periods. Development of water efficient, high yielding crop varieties	

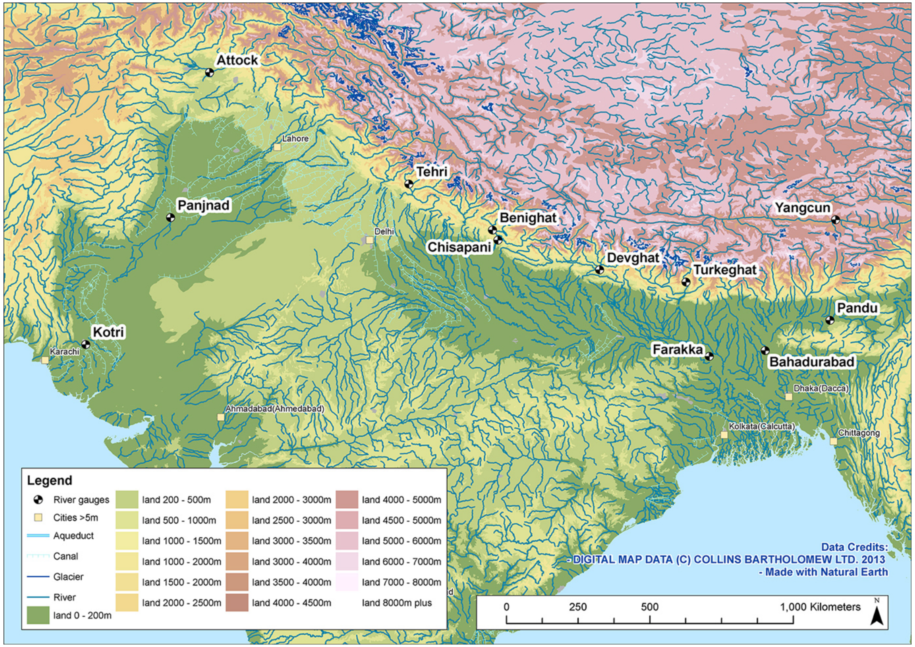

Figure 1. A map showing the locations of the river gauges used in this analysis.

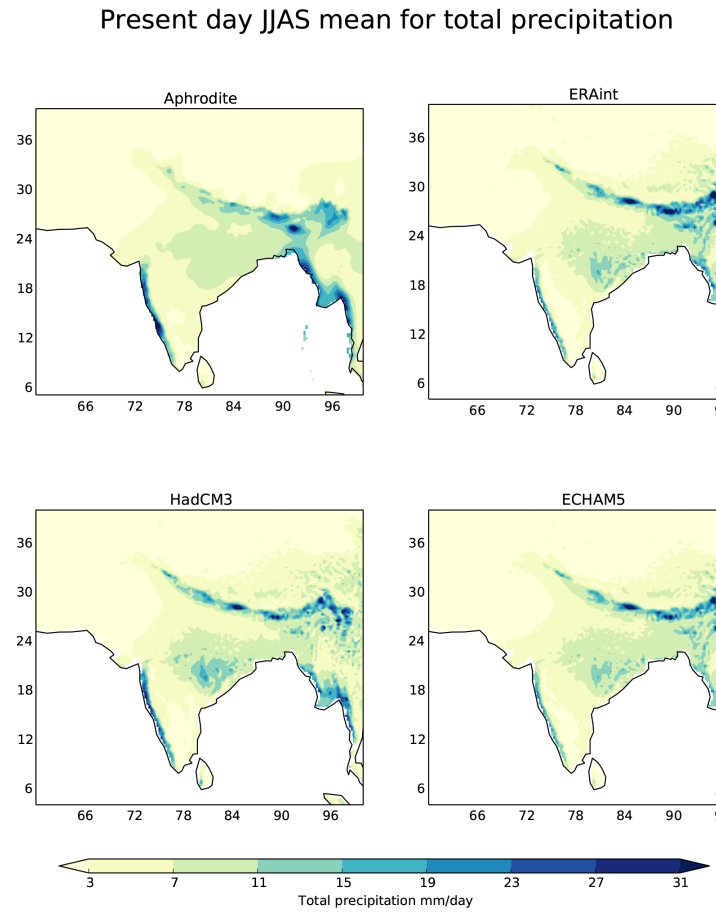

Figure 2. The spatial distribution of the seasonal mean total precipitation for the monsoon period (June, July, August, September) for APHRODITE observations (top left), ERAint (top right), HadCM3 (bottom left) and ECHAM5 (bottom right).

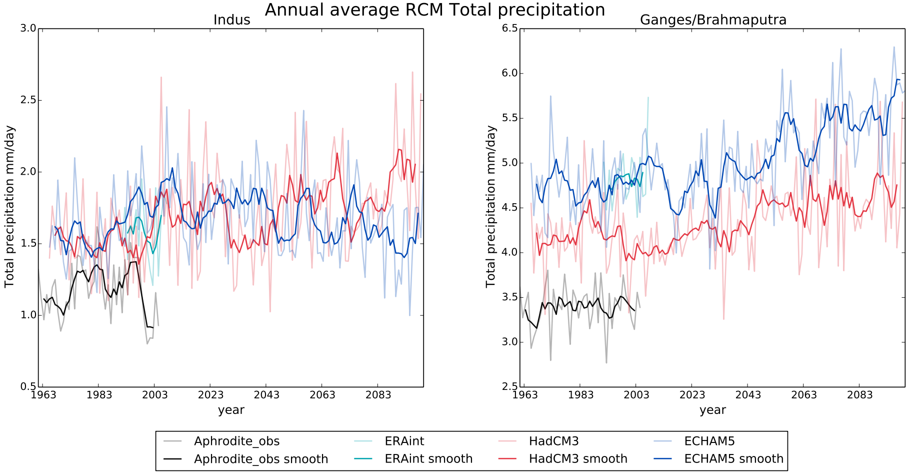

Figure 3. Annual mean total precipitation for the Indus (left) and Ganges/Brahmaputra (right) catchments for each model run (HadCM3 – red, ECHAM5 – blue, ERAint – cyan lines) plotted against APHRODITE observations (black line).

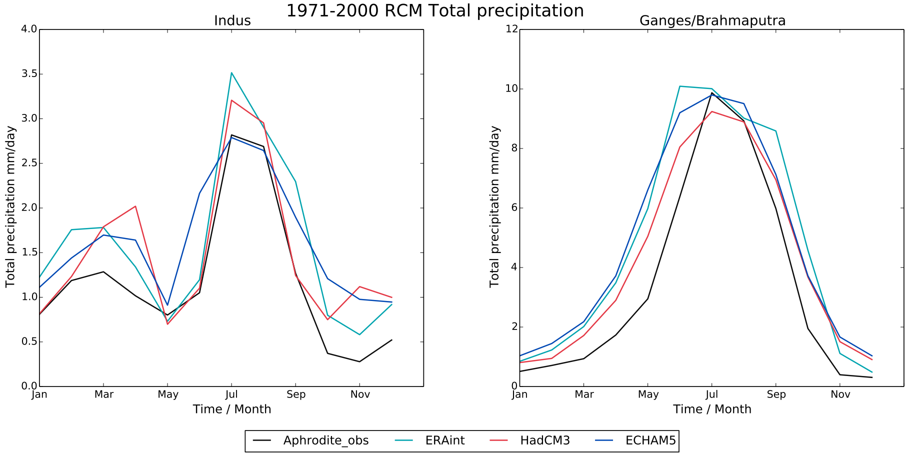

Figure 4. Seasonal cycle of total precipitation for the Indus (left) and Ganges/Brahmaputra (right) catchments for each model run (HadCM3 – red, ECHAM5 – blue, ERAint – cyan lines) plotted against APHRODITE observations (black line).

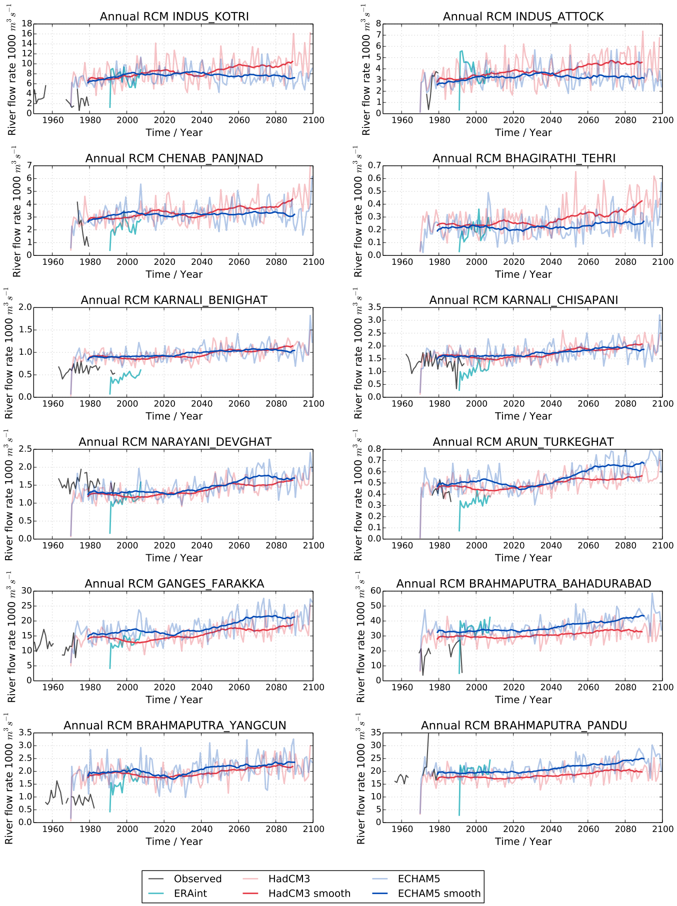

Figure 5. Timeseries of river flows showing available observations (black) and RCM runs (HadCM3 – red, ECHAM5 – blue, ERAint – cyan lines) from 1971–2100. Paler lines are annual averages and darker lines are a rolling smoothed average.

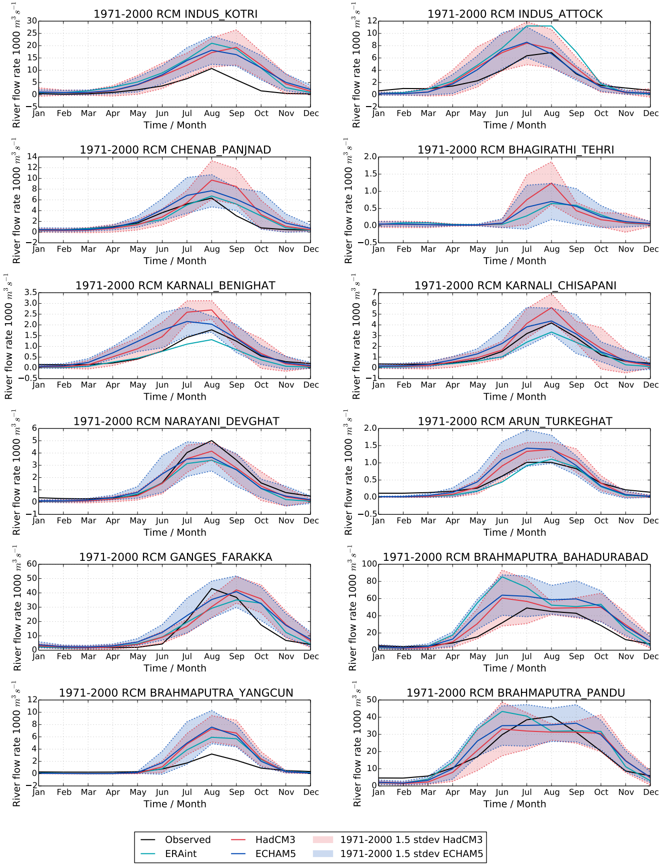

Figure 6. Seasonal cycle of river flow at individual river gauges; observed (black solid line) and for each of the RCMs (HadCM3 – red, ECHAM5 – blue, ERAint – cyan lines) for 1971–2000; with shaded regions showing 1.5 SD from the mean for the two simulations for the same period.

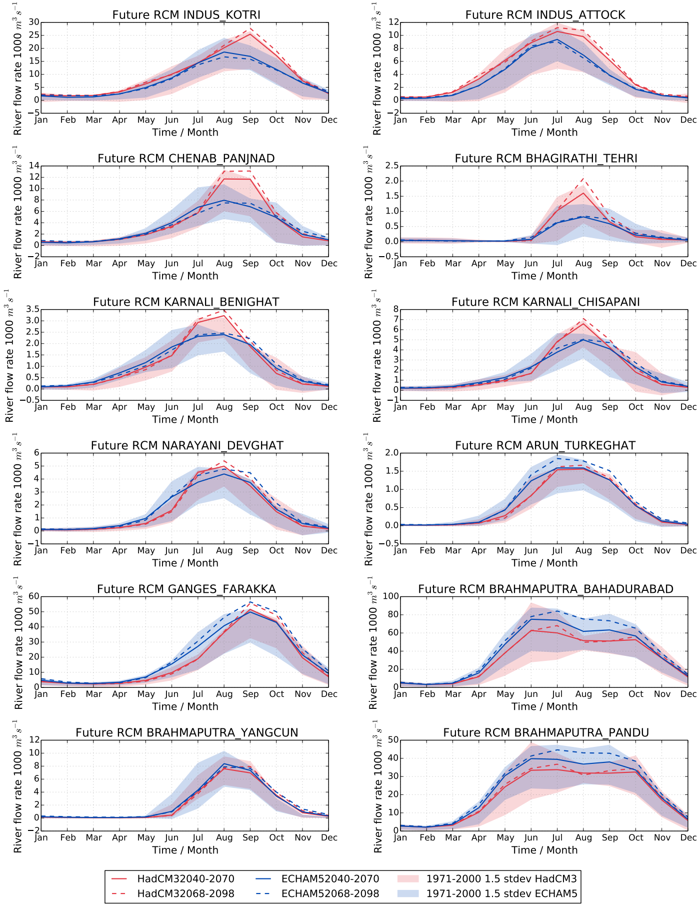

Figure 7. Seasonal cycle of river flow in each of the RCMs (HadCM3 – red, ECHAM5 – blue) for the two future periods: 2050s (solid lines) and 2080s (dashed lines), with shaded regions showing 1.5 SD from the mean for 1971–2000 for each river gauge.

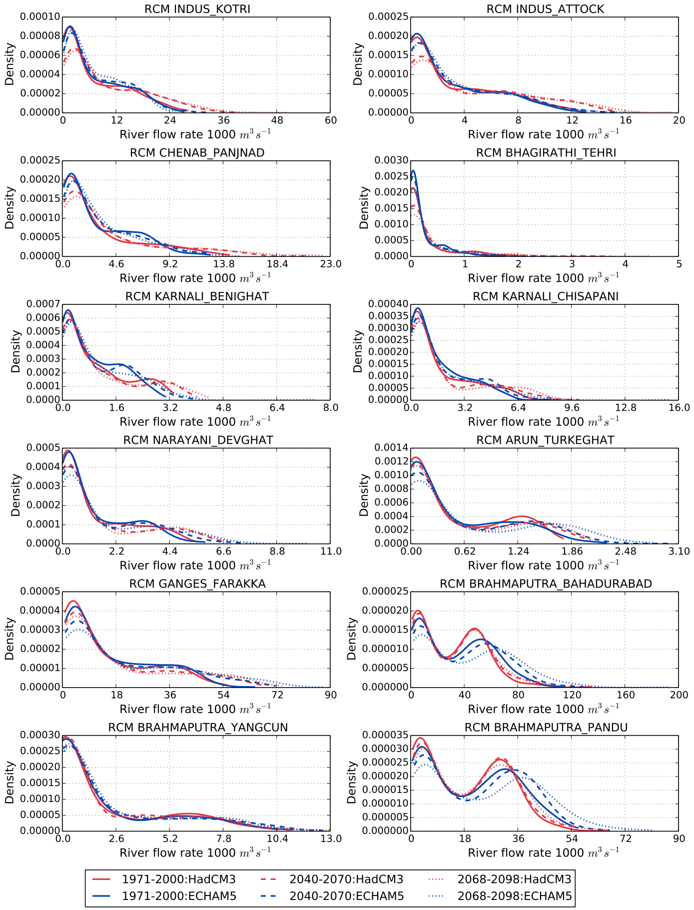

Figure 8. The distribution of the river flow in the HadCM3 and ECHAM5 (HadCM3 – red, ECHAM5 – blue) runs for three periods: historical (1971–2000 – solid lines) and two future periods (2050s – dashed lines and 2080s – dotted lines) plotted as a pdf for each river gauge.

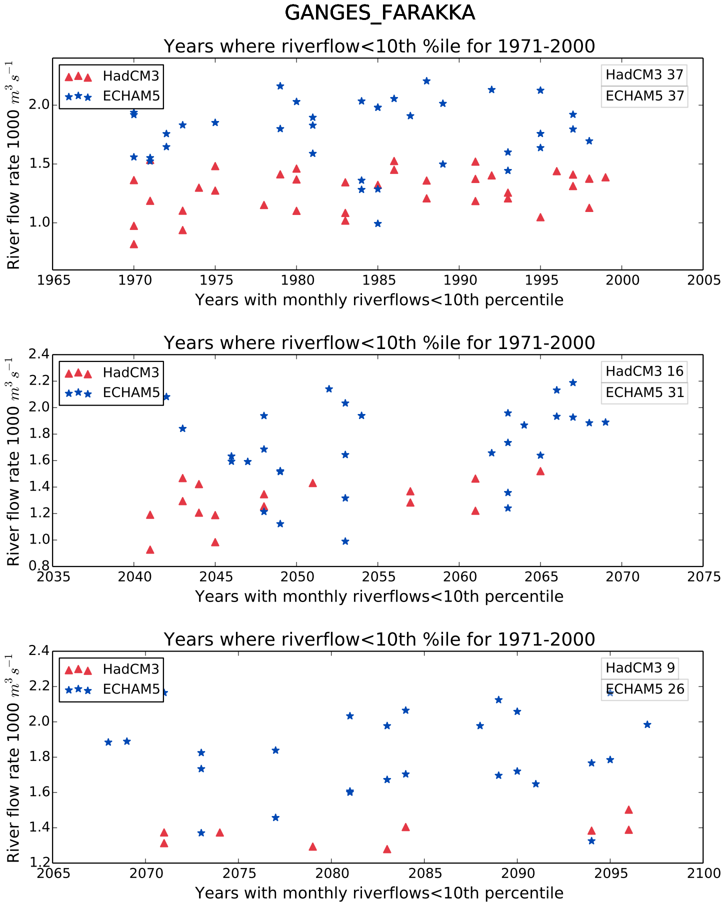

Figure 9. Comparison of the lowest 10 % of river flows at the Farakka barrage on the Ganges river against the 10th percentile for the 1971–2000 period for 1971–2000 (top), 2050s (middle) and 2080s (bottom) for HadCM3 (red triangles) and ECHAM5 (blue stars).

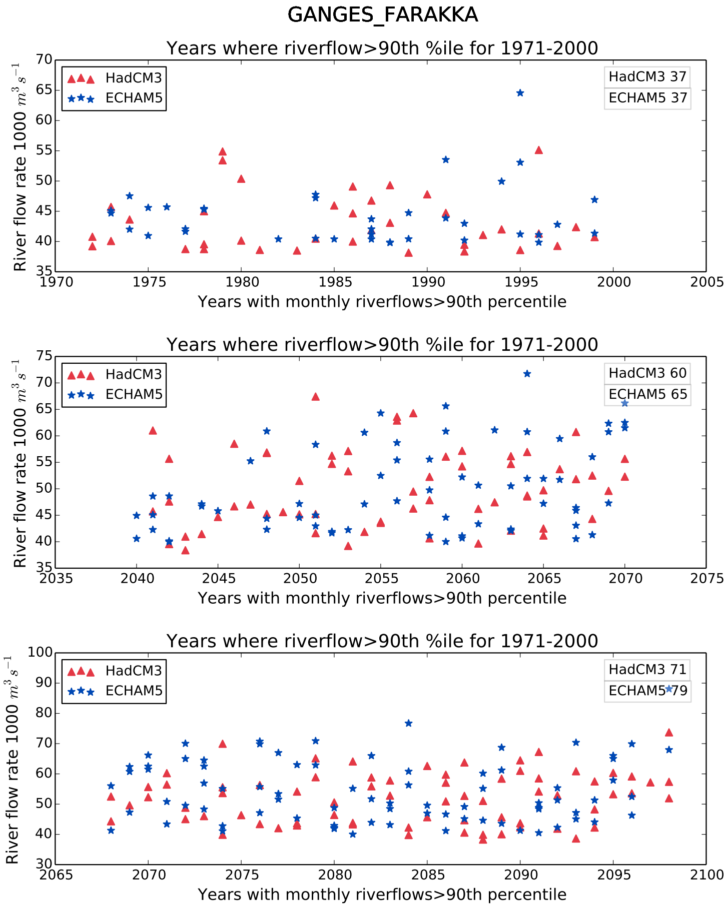

Figure 10. Comparison of the highest 10 % of river flows at the Farakka barrage on the Ganges river against the 90th percentile for the 1971–2000 period for 1971–2000 (top), 2050s (middle) and 2080s (bottom) for HadCM3 (red triangles) and ECHAM5 (bluen stars).

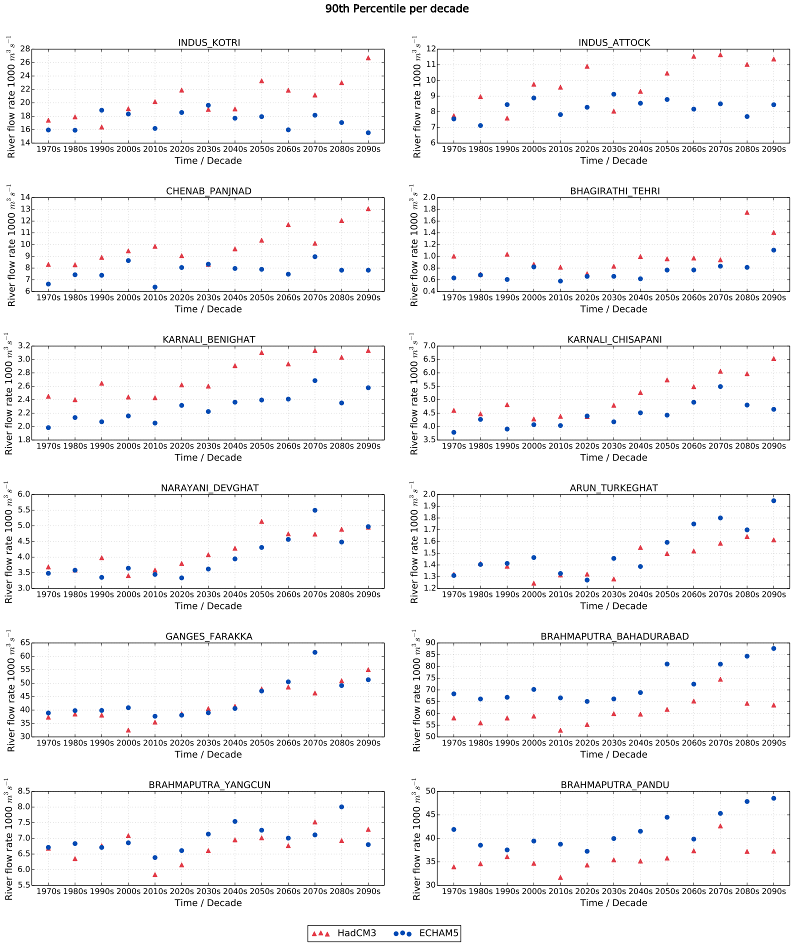

Figure 11. The 90th percentile of river flow for each decade for HadCM3 (red triangles) and ECHAM5 (blue circles) for each river gauge.